



Thermal analysis and prediction of phase equilibria in the $\text{TiO}_2\text{--Bi}_2\text{O}_3$ system

Jaqueline Lopez-Martinez^a, Antonio Romero-Serrano^{a,*}, Aurelio Hernandez-Ramirez^a, Beatriz Zeifert^a, Carlos Gomez-Yañez^a, Roberto Martinez-Sanchez^b

^a Metallurgy and Materials Department, Instituto Politecnico Nacional-ESIQIE, Apdo. P. 118-431, 07051 Mexico D.F, Mexico

^b CIMAV, Av. Miguel de Cervantes 120, Chihuahua C.P.31109, Mexico

ARTICLE INFO

Article history:

Received 9 July 2010

Received in revised form

25 November 2010

Accepted 7 January 2011

Available online 18 January 2011

Keywords:

$\text{TiO}_2\text{--Bi}_2\text{O}_3$ system

Thermodynamic prediction

Thermal analysis

ABSTRACT

A thermodynamic study on the $\text{TiO}_2\text{--Bi}_2\text{O}_3$ system was carried out using differential thermal analysis (DTA) and X-Ray diffraction (XRD) techniques covering the composition range from 65 to 90 mol% Bi_2O_3 . From the XRD results the only two intermediate compounds in the Bi_2O_3 rich region were $\text{Bi}_4\text{Ti}_3\text{O}_{12}$ and $\text{Bi}_{12}\text{TiO}_{20}$. The $\text{Bi}_4\text{Ti}_3\text{O}_{12}$ phase presents the well known plate-like morphology. The experimentally determined phase transition temperatures with DTA technique were compared with thermodynamic calculated results and good agreement was obtained. The DTA results also showed that the limit of the peritectic reaction between liquid and $\text{Bi}_4\text{Ti}_3\text{O}_{12}$ occurs approximately at 90 mol% Bi_2O_3 .

The phase diagram of the $\text{TiO}_2\text{--Bi}_2\text{O}_3$ system was calculated using a quasichemical model for the liquid phase. The thermodynamic properties of the intermediate compounds were estimated from the data of TiO_2 and Bi_2O_3 pure solids. In this manner, data for this binary system have been analysed and represented with a small adjustable parameter for the liquid phase.

© 2011 Elsevier B.V. All rights reserved.

1. Introduction

It has been reported that bismuth titanates exhibit a number of interesting properties, including dielectric, piezoelectric, electro-optical, elasto-optical and photoconductivity properties [1,2]. The sillenite-type compound $\text{Bi}_{12}\text{TiO}_{20}$ and the ferroelectric compound $\text{Bi}_4\text{Ti}_3\text{O}_{12}$ have been used in capacitors, transducers and sensors. Several methods have been developed to prepare these bismuth titanates, however the $\text{TiO}_2\text{--Bi}_2\text{O}_3$ phase diagram remains unclear in some ranges of compositions.

Bruton [3] reported that the $\text{Bi}_{12}\text{TiO}_{20}$ compound melts incongruently at 1148 K where it decomposes into Bi_2O_3 and $\text{Bi}_4\text{Ti}_3\text{O}_{12}$. The bismuth-rich compound has also been identified as $\text{Bi}_{12}\text{TiO}_{20}$ by Levin and Roth [4] who suggested that it is congruently melting. Morrison [5] also concluded that the congruent melting is favored but there is a small departure from congruent melting. According to the published phase diagram data by Speranskaya et al. [6], three incongruently melting compounds exist in the $\text{TiO}_2\text{--Bi}_2\text{O}_3$ system: $\text{Bi}_4\text{Ti}_3\text{O}_{12}$ (peritectic melting temperature at 1483 K), the bismuth-rich phase $\text{Bi}_8\text{TiO}_{14}$ (peritectic melting temperature at about 1138 K) and the titanium-rich compound $\text{Bi}_2\text{Ti}_4\text{O}_{11}$ (peri-

itectic melting temperature at 1548 K). Miyazawa and Tabata [7] studied the hypo-peritectic region of stoichiometric $\text{Bi}_{12}\text{TiO}_{20}$ by means of lattice parameters measurements of crystals grown from a Bi_2O_3 -rich solution and found the existence of a solid solution with retrograde solidus curve at about 13.85 mol% TiO_2 . Masuda et al. [8] reported the bismuth-rich phases $\text{Bi}_8\text{TiO}_{14}$ and $\text{Bi}_{12}\text{TiO}_{20}$.

It is clear that bismuth titanates crystals present great potential for applications but they have to be grown in a reproducible way to ensure the best performance. In this regard a reliable phase diagram is necessary. Thus, the objective of the present study is to investigate the phase diagram in the Bi_2O_3 -rich region of the $\text{TiO}_2\text{--Bi}_2\text{O}_3$ binary system using differential thermal analysis (DTA) and X-Ray diffraction. We aim to determine experimentally which Bi-rich compounds ($\text{Bi}_8\text{TiO}_{14}$ and $\text{Bi}_{12}\text{TiO}_{20}$) can be formed from the liquid phase. A thermodynamic calculation of the binary system is also carried out in this work using the modified quasichemical model for the liquid phase [9].

2. Experimental

The oxide samples were prepared from reagent-grade TiO_2 and Bi_2O_3 oxides (purity higher than 99.9%) previously ground to +45–74 μm particle size. Four different compositions were prepared in the binary system $\text{TiO}_2\text{--Bi}_2\text{O}_3$: 65, 75, 85.71 and 90 mol% Bi_2O_3 . It is worth to note that the sample with 85.71% Bi_2O_3 corresponds to the stoichiometric composition of the $\text{Bi}_{12}\text{TiO}_{20}$ compound. 20 g of each oxide system were prepared as follows: the powders were homogeneously mixed and placed in a platinum cru-

* Corresponding author. Tel.: +55 5729 6000x54217; fax: +55 5729 6000x55270.

E-mail addresses: jacky-411@hotmail.com (J. Lopez-Martinez),

romeroipn@hotmail.com (A. Romero-Serrano), aurelioh@hotmail.com

(A. Hernandez-Ramirez), bzeifert@yahoo.com (B. Zeifert), cgomezzy@ipn.mx

(C. Gomez-Yañez), roberto.martinez@cimav.edu.mx (R. Martinez-Sanchez).

cible which was protected by an alumina crucible inside an electric furnace. Each mixture was heated up to 1473 K and remained in that temperature for 4 h, to ensure complete homogenization; temperature was measured with an R-type thermocouple (Pt–Pt, 13%Rh). The samples were left inside the furnace and the temperature was slowly decreased (2 K/min) up to room temperature.

Samples of each system were crushed into fine powders and characterized by X-ray diffraction (XRD Bruker D8 Focus) and scanning electron microscopy coupled with energy dispersive spectroscopy (SEM-EDS, FEI model Quanta 3D FEG). The DTA measurements were performed on a DTA-TGA TA Instruments SDT 2960. Alumina crucibles were used and measurements were performed under argon atmosphere. Samples weighting between 80 and 140 mg were investigated using the heating rate of 5 K/min.

3. Thermodynamic model for the TiO_2 – Bi_2O_3 liquid system

For the liquid phase we used the modified quasichemical model proposed by Pelton and Blander [9]. A detailed development was given previously [9], only a brief summary will be presented here. In a binary solution TiO_2 – Bi_2O_3 melt, one might identify the “1” and “2” particles with Ti and Bi which mix on a cation quasi-lattice. In this system “1” and “2” particles mix substitutionally, we consider the formation of two 1–2 nearest-neighbour pairs from a 1–1 and a 2–2 pair.

$$[1-1] + [2-2] = 2[1-2] \quad (1)$$

Let the molar enthalpy and non-configurational entropy change for reaction (1) be ω and η , respectively. If $(\omega - T\eta) = 0$, then the solution is an ideal solution. If $(\omega - T\eta)$ is very negative, then 1–2 pairs predominate and the solution is ordered. Let us consider X_1 and X_2 as the mole fractions. “Equivalent Fractions”, Y_1 and Y_2 , are defined as:

$$Y_1 = \frac{b_1 X_1}{b_1 X_1 + b_2 X_2} = 1 - Y_2 \quad (2)$$

where b_1 and b_2 are constants chosen so as that the Gibbs free energy minimum occurs at the experimental composition, and so that the configurational entropy is zero at this composition when $(\omega - T\eta) = -\infty$. It was shown [9] that the appropriate choice of constants are $b_{\text{BiO}_{1.5}} = 1.0331$ and $b_{\text{TiO}_2} = 1.3774$. Letting X_{11} , X_{22} and X_{12} be the fractions of each type of pair in solution and z the coordination number, one obtains a quasichemical equilibrium constant for reaction (1)

$$\frac{X_{12}^2}{X_{11} X_{22}} = 4 \exp \left[\frac{-2(\omega - \eta T)}{zRT} \right] \quad (3)$$

Two mass-balance equations may be written

$$2Y_1 = 2X_{11} + X_{12} \quad (4)$$

$$2Y_2 = 2X_{22} + X_{12} \quad (5)$$

For a given value of $(\omega - T\eta)$, Eqs. (2)–(5) can be solved at any composition to give X_{11} , X_{22} and X_{12} . The molar Gibbs free energy of mixing is given by:

$$\begin{aligned} \Delta g^{\text{mix}} &= RT(X_1 \ln X_1 + X_2 \ln X_2) \\ &+ \frac{RTz(b_1 X_1 + b_2 X_2)}{2} \times \left(X_{11} \ln \frac{X_{11}}{Y_1^2} + X_{22} \ln \frac{X_{22}}{Y_2^2} + X_{12} \ln \frac{X_{12}}{2Y_1 Y_2} \right) \\ &+ \frac{b_1 X_1 + b_2 X_2}{2} X_{12} (\omega - \eta T) \end{aligned} \quad (6)$$

where the configurational entropy has been approximated by a one-dimensional Ising model [9]. In order to permit the precise

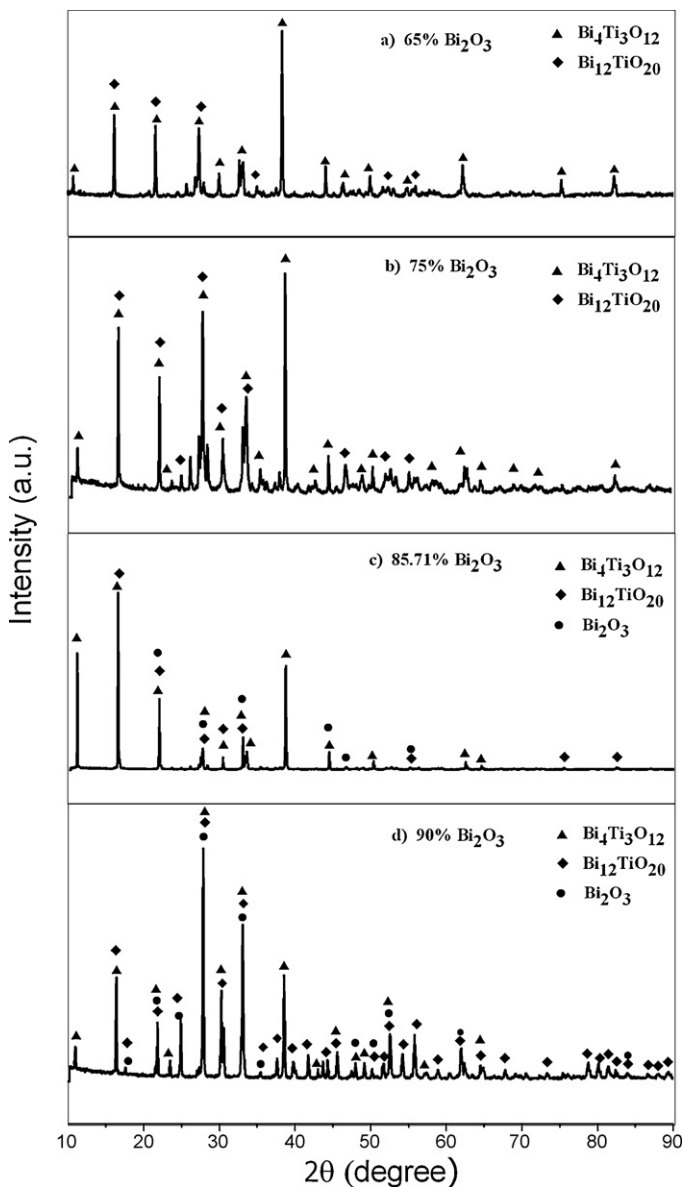


Fig. 1. XRD patterns of TiO_2 – Bi_2O_3 mixtures with compositions from 65 to 90 mol% Bi_2O_3 .

representation of the experimental data, ω and η are expanded as a polynomial in the equivalent fractions

$$\omega = \omega_0 + \omega_1 Y_2 + \omega_2 Y_2^2 + \dots \quad (7)$$

$$\eta = \eta_0 + \eta_1 Y_2 + \eta_2 Y_2^2 + \dots \quad (8)$$

The coefficients ω_i and η_i are the parameters of the model which are obtained by optimization of the experimental data.

4. Results and discussion

4.1. X-ray diffraction

X-ray diffraction patterns of samples with 65, 75, 85.71 and 90 mol% Bi_2O_3 are shown in Fig. 1. From the XRD patterns obtained in this work it can be concluded that only the phases Bi_2O_3 , $\text{Bi}_4\text{Ti}_3\text{O}_{12}$ and $\text{Bi}_{12}\text{TiO}_{20}$ are involved in the studied composition range. Speranskaya et al. [6] reported that the $\text{Bi}_8\text{TiO}_{14}$ compound

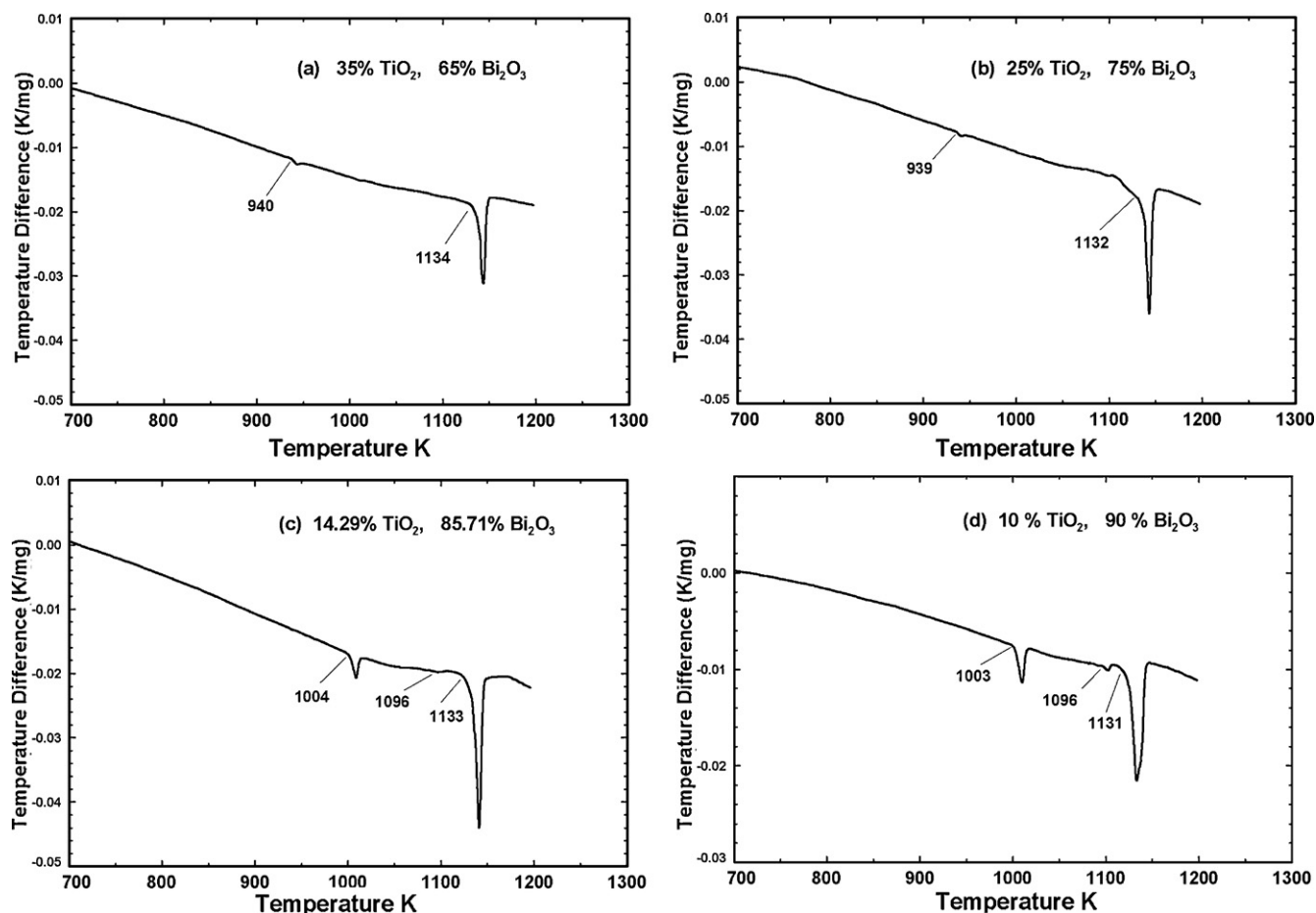
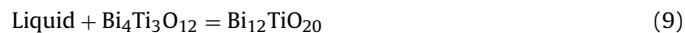


Fig. 2. DTA heating curves for TiO_2 - Bi_2O_3 mixtures with compositions from 65 to 90 mol% Bi_2O_3 .

was formed between the compounds $\text{Bi}_4\text{Ti}_3\text{O}_{12}$ and $\text{Bi}_{12}\text{TiO}_{20}$; however, we did not detect the formation of such a compound in our samples. Bruton [3] and Levin and Roth [4] did not find the phase $\text{Bi}_8\text{TiO}_{14}$ either. The main problem, in this analysis is that the patterns corresponding to the phases Bi_2O_3 , $\text{Bi}_4\text{Ti}_3\text{O}_{12}$ and $\text{Bi}_{12}\text{TiO}_{20}$ (JCPDS files 27-0053, 12-0213 and 34-0097, respectively) are very similar. Most of the peaks in the patterns (Fig. 1) are overlapped signals coming from the mentioned phases. The peaks that correspond only to $\text{Bi}_4\text{Ti}_3\text{O}_{12}$ are at $2\theta = 11^\circ$ and $2\theta = 38.7^\circ$. The last peak diminishes in intensity when the amount of Bi_2O_3 is increased, as expected; however, it does not disappear for the samples with 85.71 and 90% Bi_2O_3 when the peritectic reaction takes place, which suggests that the kinetics of transformation during cooling is rather slow. In fact $\text{Bi}_{12}\text{TiO}_{20}$ is produced by a peritectic reaction, where liquid and $\text{Bi}_4\text{Ti}_3\text{O}_{12}$ should react stoichiometrically at 85.71% Bi_2O_3 (Fig. 1c) to produce $\text{Bi}_{12}\text{TiO}_{20}$.



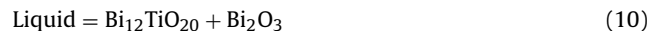
4.2. DTA results

Fig. 2 shows the DTA heating curves for TiO_2 - Bi_2O_3 mixtures of different compositions (65, 75, 85.71 and 90 mol% Bi_2O_3). During the DTA test insignificant mass losses were observed (less than 0.8%). The following general remarks were made in the DTA measurements:

(a) Samples with 65 and 75% Bi_2O_3 show two endothermic peaks. The first peak is about at 940 K which corresponds to the transition of the crystalline structure of $\text{Bi}_4\text{Ti}_3\text{O}_{12}$. The second is a

quite wide peak at about 1134 K which can be ascribed to the peritectic reaction, Eq. (9).

(b) The sample with 85.71% Bi_2O_3 corresponds with the stoichiometric composition of the $\text{Bi}_{12}\text{TiO}_{20}$ compound and the thermogram must present only the peak for the peritectic transformation, at about 1133 K. However, we obtained other two small peaks, the first peak is at 1004 K and may correspond to the structure change of Bi_2O_3 from monoclinic to cubic; the second peak is about at 1096 K which can be ascribed to the eutectic transformation:



This incongruity may be due to the lack of both, the appropriate homogenization time and cooling rate to obtain only the $\text{Bi}_{12}\text{TiO}_{20}$ compound during the peritectic reaction (9).

(c) Fig. 2d shows three thermal effects in the thermogram for the sample with 90% Bi_2O_3 : a thermal arrest corresponds to the structure change of Bi_2O_3 from monoclinic to cubic at 1003 K, the second one corresponds to the eutectic (Eq. (10)) at about 1096 K, and the last one can be ascribed to the peritectic transformation (Eq. (9)) at 1131 K.

The DTA results for the sample with 90% Bi_2O_3 help us to locate approximately the limit of the peritectic reaction between liquid and $\text{Bi}_4\text{Ti}_3\text{O}_{12}$. Levin and Roth [4] and Morrison [5] reported that the peritectic line is from 40 mol% Bi_2O_3 (the composition of $\text{Bi}_4\text{Ti}_3\text{O}_{12}$) up to about 86% Bi_2O_3 . Miyazawa and Tabata [7] reported that the peritectic composition must lie close to 89.25 mol% Bi_2O_3 which is in agreement with our DTA results.

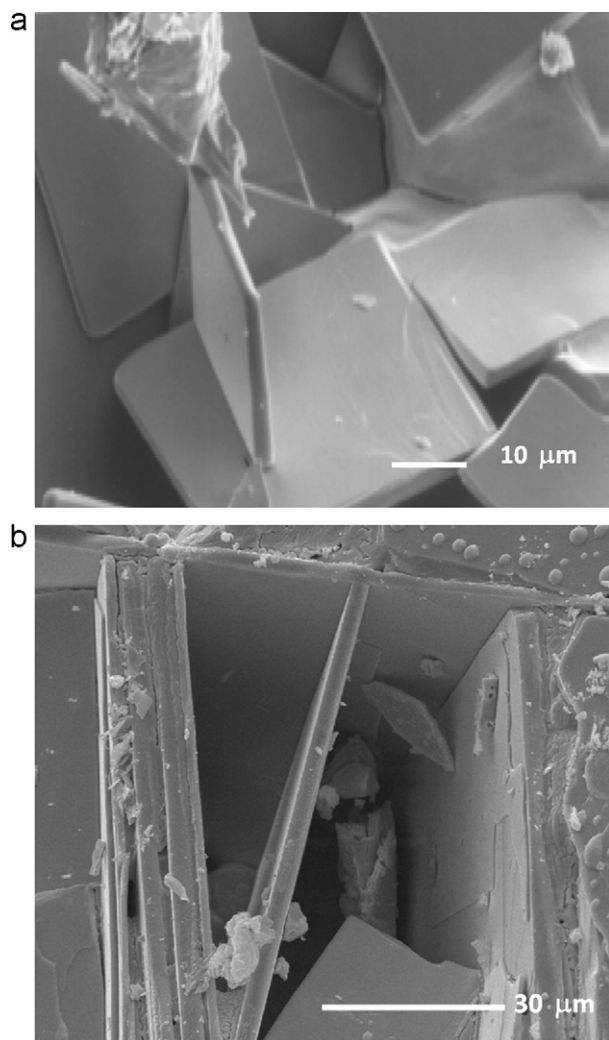


Fig. 3. SEM micrographs of sample with 75 mol% Bi_2O_3 . The platelets-like grains correspond to $\text{Bi}_4\text{Ti}_3\text{O}_{12}$.

4.3. SEM results

Fig. 3 shows two SEM micrographs of the sample with 75% Bi_2O_3 . These figures show plate-like morphology, with a size of about $3\ \mu\text{m}$ in thickness and between 40 and $60\ \mu\text{m}$ in width. Semiquantitative EDS analysis of these crystals were carried out and the Bi/Ti ratio was calculated of at least five measurements. The results show a value that corresponds to crystals of $\text{Bi}_4\text{Ti}_3\text{O}_{12}$, which is in agreement with the X-Ray diffraction results. Jardiel et al. [10] reported that the bismuth titanate ($\text{Bi}_4\text{Ti}_3\text{O}_{12}$) based ceramics reflects the microstructure showing big platelets-like grains growing preferentially in a given plane.

The Bi_2O_3 crystallizes in the monoclinic crystal system with lattice parameters $a = 5.848$, $b = 8.166$, $c = 7.51$; ($\alpha = \gamma = 90^\circ \neq \beta$). The $\text{Bi}_{12}\text{TiO}_{20}$ crystallizes in the body centered cubic crystal system with lattice parameters $a = 10.1739$ ($\alpha = \beta = \gamma = 90^\circ$). The $\text{Bi}_4\text{Ti}_3\text{O}_{12}$ crystallizes in the orthorhombic crystal system with lattice parameters $a = 5.41$, $b = 5.448$, $c = 32.84$ ($\alpha = \beta = \gamma = 90^\circ$). The differences on the habit of the crystals and their quite similar morphologies make difficult to use the SEM analysis to determine which phases are present after the invariant reaction and prove that such a reaction is completely carried out.

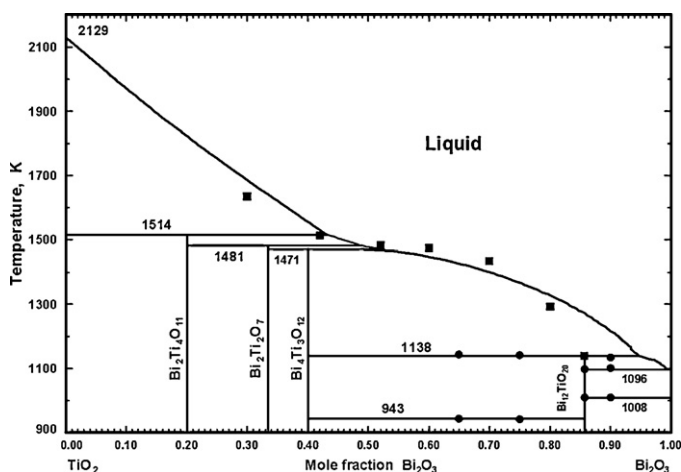


Fig. 4. Calculated optimized TiO_2 - Bi_2O_3 system. Experimental points: (■) Ref. [8]; (●) this work.

4.4. Thermodynamic results

The experimental data of heat capacities of TiO_2 and Bi_2O_3 are available, so the standard Gibbs free energy function can be described by:

$$g^\circ = a + bT + cT^{-2} + dT \ln T + eT^{-1} \quad (11)$$

According to our results and the phase diagrams reported previously, there exist four intermediate compounds in the TiO_2 - Bi_2O_3 . Unfortunately, there is no thermodynamic data for these compounds. The Gibbs free energy function for the intermediate compounds is estimated according to the expression:

$$g_{x\text{TiO}_2 \cdot y\text{Bi}_2\text{O}_3}^\circ = x g_{\text{TiO}_2}^\circ + y g_{\text{Bi}_2\text{O}_3}^\circ + E + FT \quad (12)$$

where x and y are 4 and 1 for $\text{Bi}_2\text{Ti}_4\text{O}_{11}$, 2 and 1 for $\text{Bi}_2\text{Ti}_2\text{O}_7$, 3 and 2 for $\text{Bi}_4\text{Ti}_3\text{O}_{12}$, 1 and 6 for $\text{Bi}_{12}\text{TiO}_{20}$. E and F are optimizable coefficients chosen to fit the experimental phase diagram. Thermodynamic parameters for the TiO_2 and Bi_2O_3 as well as the optimized properties of the intermediate compounds are given in Table 1.

The calculated optimized phase diagram is shown in Fig. 4 where compositions are given in terms of the components TiO_2 - Bi_2O_3 instead of TiO_2 - $\text{BiO}_{1.5}$. The assessment is based largely upon the phase diagram reported by Masuda et al. [8] who used differential thermal analysis and it is in substantial agreement with that of Miyazawa and Tabata [7], except for the formation of the $\text{Bi}_8\text{TiO}_{14}$ compound. The reported experimental phase diagrams [7,8] were used for determining the coefficients in Eqs. (7) and (8) which best reproduce all of the data. The following expressions for ω and η were found for the liquid:

$$\omega = -5600 + 2000 Y_{\text{BiO}_{1.5}}^3 \text{ J mol}^{-1} \quad (13)$$

$$\eta = Y_{\text{BiO}_{1.5}} + 5.0 Y_{\text{BiO}_{1.5}}^3 \text{ J mol}^{-1} \text{ K}^{-1} \quad (14)$$

The experimental and calculated temperatures of the invariant reactions and the compositions of Bi_2O_3 in the liquid phases are listed in Table 2. Predicted results from this work are in good agreement with those published by Masuda et al. [8], except in the liquidus near Bi_2O_3 . Even though, Miyazawa and Tabata [7], Masuda et al. [8] and Speranskaya et al. [6] reported the liquidus with dashed lines which means that there exists high experimental uncertainties in this liquidus line.

Table 1
Standard Gibbs free energy of the compounds in the TiO₂–Bi₂O₃ system.

	$g_{\circ} = a + bT + cT^{-2} + dT \ln T + eT^{-1} \text{ J mol}^{-1}$				
	<i>a</i>	<i>b</i>	<i>c</i>	<i>d</i>	<i>e</i>
Bi ₂ O ₃ (s)	–572,120.78	799.39145	0.0	–146.440	0.0
Bi ₂ O ₃ (l)	–519,174.35	794.9820	0.0	–152.71602	0.0
TiO ₂ (s)	–976,986.65	484.740378	–67,156,778.7	–77.837621	1,683,920.5
TiO ₂ (l)	–930,962.65	463.132871	–67,156,778.7	–77.837621	1,683,920.5
Bi ₂ Ti ₄ O ₁₁ (s)	–4,519,667.383	2738.3530	–268,627,112	–457.790486	6,735,682.0
Bi ₂ Ti ₂ O ₇ (s)	–2,563,294.084	1768.8722	–134,313,556	–302.115243	3,367,841.0
Bi ₄ Ti ₃ O ₁₂ (s)	–4,147,581.515	3053.0040	–201,470,334	–526.392864	5,051,761.5
Bi ₁₂ TiO ₂₀ (s)	–4,449,491.345	5281.0891	–67,156,778.7	–956.477621	1,683,920.5

Table 2
Experimental and calculated invariant equilibria of TiO₂–Bi₂O₃ system.

Reaction	Masuda et al. [8]		Calculated, this work	
	T, K	mol% Bi ₂ O ₃ ^a	T, K	mol% Bi ₂ O ₃ ^a
L + TiO ₂ = Bi ₂ Ti ₄ O ₁₁	1513	42.43	1514	43.22
L + Bi ₂ Ti ₄ O ₁₁ = Bi ₂ TiO ₇	1483	50.65	1481	48.89
L + Bi ₂ Ti ₂ O ₇ = Bi ₄ Ti ₃ O ₁₂	1473	58.36	1471	51.64
L + Bi ₄ Ti ₃ O ₁₂ = Bi ₁₂ TiO ₂₀	1138	85.91	1138	94.73
L = Bi ₁₂ TiO ₂₀ + Bi ₂ O ₃	1108	97.01	1096	99.40

^a mol% of Bi₂O₃ in liquid.

5. Conclusions

A study on the TiO₂–Bi₂O₃ system was carried out using differential thermal analysis (DTA) and X-Ray diffraction (XRD) techniques covering the composition range from 65 to 90 mol% Bi₂O₃. From the XRD results the only two intermediate compounds in the Bi₂O₃ rich region were Bi₄Ti₃O₁₂ and Bi₁₂TiO₂₀. The Bi₄Ti₃O₁₂ phase presents a plate-like morphology, with a size of about 3 μm in thickness and between 40 and 60 μm in width. The DTA results show that the limit of the peritectic reaction between liquid and Bi₄Ti₃O₁₂ is at approximately 90 mol% Bi₂O₃ which is in agreement with the reported results in the literature.

The TiO₂–Bi₂O₃ phase diagram was thermodynamically assessed in the present work. The quasichemical model was used for the liquid phase. The Gibbs free energy functions for the intermediate compounds were estimated from the properties of the TiO₂ and Bi₂O₃ pure solids. The calculated phase diagram is in good agreement with the experimental results; however, further experimental study of the liquidus line in the Bi₂O₃ rich region is required.

Acknowledgments

The authors wish to thank the Institutions CONACyT, SNI, COFAA and IPN for their permanent assistance to the Process Metallurgy Group at ESIQIE-Metallurgy and Materials Department. RMS wishes to thank CIMAV.

References

- [1] L. Gao, Y. Huang, L. Liu, T. Liu, C. Liu, F. Zhou, X. Wan, J. Mater. Sci. 43 (2008) 6267–6271.
- [2] Z. Bian, J. Ren, J. Zhu, S. Wang, Y. Lu, H. Li, Appl. Catal. B: Environ. 89 (2009) 577–582.
- [3] T.M. Bruton, J. Solid State Chem. 9 (1974) 173–175.
- [4] E.M. Levin, R.S. Roth, J. Res. Natl. Bur. Stand. Sect. A 68 (1964) 197–206.
- [5] A.D. Morrison, Ferroelectrics 2 (1971) 59–62.
- [6] E.I. Speranskaya, I.S. Rez, L.V. Kozlova, V.M. Skorikov, V.I. Slavov, J. Inorg. Mater. (1965) 213–216.
- [7] S. Miyazawa, T. Tabata, J. Cryst. Growth 191 (1998) 512–516.
- [8] Y. Masuda, H. Masumoto, A. Baba, T. Goto, T. Hirai, Jpn. J. Appl. Phys. Part 1 31 (1992) 3108–3112.
- [9] A.D. Pelton, M. Blander, Metall. Trans. B 17B (1986) 805–815.
- [10] T. Jardiel, A.C. Caballero, J.F. Fernández, M. Villegas, J. Eur. Ceram. Soc. 26 (2006) 2823–2826.